A multiaxial growth analysis of stable isotopes in the modern shell of *Saxidomus gigantea*: Implications for sclerochronology studies

Andrew W. Kingston

Department of Earth and Ocean Sciences, University of British Columbia, 6339 Stores Road, Vancouver, British Columbia, Canada V6T 1Z4

Darren R. Gröcke

Department of Earth Sciences, Durham University, Science Laboratories, South Road, Durham DH1 3LE, UK (d.r.grocke@durham.ac.uk)

Meghan Burchell

Department of Anthropology, McMaster University, Hamilton, Ontario, Canada L8S 4L9

[1] Stable-isotope ratios of two modern *Saxidomus gigantea* specimens from Namu, British Columbia, are presented to show intraspecimen and interspecimen isotopic variation. Isotopic profiles ($\delta^{13}C_{shell}$, $\delta^{18}O_{shell}$) were generated along the axis of maximum growth. The profiles show that analogous seasonal variation is recorded in $\delta^{18}O_{shell}$; however, significant variability is recorded in $\delta^{13}C_{shell}$. We suggest this is caused by differences in metabolic activity between individuals. Intrashell variability along a growth horizon shows good reproducibility in $\delta^{13}C_{shell}$ but significant variability in $\delta^{18}O_{shell}$, especially at the sinistral margin. A multiaxial growth analysis generated several profiles from a single valve. Similar seasonal variations are recorded in $\delta^{18}O_{shell}$ along all axes. $\delta^{13}C_{shell}$ show significantly less covariation, possibly related to internal metabolic activity. This study highlights that $\delta^{18}O_{shell}$ profiles generated from any portion of the shell can be used to evaluate seasonal fluctuations and may be excellent to evaluate types and rates of shell growth.

1. Introduction

[2] Bivalves are becoming popular materials for reconstructing climatic and environmental condi-tions through the application of stable-isotope and trace element geochemistry. Previous studies have shown that the stable-isotope ratio ($\delta^{13}C_{shell}$, $\delta^{18}O_{shell}$) of bivalve shell carbonate can success-

fully record environmental conditions, such as temperature and salinity, and therefore have been applied to investigate seasonal variability [*Shackleton*, 1973; *Krantz et al.*, 1987; *Goodwin et al.*, 2003a; *Schöne et al.*, 2006]. These studies have typically used complete valves that are cross-sectioned along their axis of maximum growth, and thus provide the most complete geochemical record through its life history. However, in some cases complete valves are not available for geochemical analysis, and at present it is not understood how stable isotope profiles appear around the concave shape of a bivalve. For example, sediment coring can fragment shells and thus only a portion of the shell is retrieved for isotopic analysis. Alternatively the shells may have become fragmented through human and/or natural depositional processes.

[3] In order to fully utilize shell material that has been fragmented either through the process of deposition or retrieving samples via coring we have investigated the distribution of stable isotopes in a single species of bivalve, *Saxidomus gigantea* (Deshayes, 1839). The possibility of shell isotope inhomogeneities is the main concern which could arise due to several reasons, including the following: (1) proximity to the location where the precipitating fluid is produced; (2) faster growth rate at the axis of maximum growth compared with adjacent areas; and (3) other undefined biological fractionation processes [e.g., *Rosenberg and Hughes*, 1991; *Goodwin et al.*, 2003a, 2003b; *Carré et al.*, 2005]. The results of this study will help contribute to the current understanding of bivalve shell stable isotope geochemistry, and whether fragmented or partial valves can be used in paleoclimatological studies. Two types of techniques have been employed in this study:

[4] 1. A Hendy-type test [*Hendy*, 1971] is a technique that is typically applied to speleothem studies in order to determine whether the speleothem is in isotopic equilibrium with its surrounding environment. In the case of speleothems the test is used to determine if processes such as limited amounts of bicarbonate in solution and/or evaporation have affected the isotopic composition of the carbonate along a growth horizon [e.g., *Lauritzen and Lundberg*, 1999]. The Hendy-type test involves taking a series of samples along a growth horizon (Figure 1a), where in principle, all the stable-isotope values should be the same if the precipitation of carbonate is in equilibrium. A similar, but lower-resolution study was conducted by *Klein et al.* [1996] on the bivalve, *Mytilus trossulus*, who

indicated significant changes in $\delta^{13}C_{shell}$ at the lateral margins, and minor changes in $\delta^{18}O_{shell}$. Recently, problems associated with sampling at the margins in speleothems have been identified, in that the difference between the drill diameter (0.5 mm) and the size of growth horizons (down to the micron scale) would mean that sampling a consistent layer would be very difficult [*Lauritzen and Lundberg*, 1999].

[5] 2. Previous studies using sclerochronological techniques have sampled along the maximum axis of growth (axis 3 in Figure 1b), in order to capture all possible time preserved in the shell. Another method in which to determine reproducibility would be to sample multiple axes of growth (Figure 1b): termed multiaxial growth analysis hereafter. Using a prominent growth line as a marker along the shell, three or more transects can be produced in which a direct comparison can be made.

2. Methods

2.1. Sampling Strategy

[6] Stable-isotope profiles of two modern *S. gigantea* specimens collected from Namu, British Columbia, Canada (16 August 2006; lat: 51.867, long: −127.867) were generated along the axis of maximum growth in order to show the cyclicity recorded in these bivalves. These samples were collected during low tide and were located within the intertidal zone. One of these modern samples (MNBC 4) was used for the Hendy-type test and multiaxial growth analysis outlined below.

2.1.1. Hendy-Type Test

[7] A traditional Hendy test is accomplished by drilling a series of samples along a time-equivalent horizon, most typically applied to the isotopic analysis of speleothems. In our Hendy-type test the left valve of a modern *S. gigantea* was used. The surficial portion of the valve (<0.5 mm) was removed using an aluminum oxide grinding stone attached to a dentist-type drill. The shell was then washed in an ultrasonic bath using deionized water. Discrete sub-samples along and beside the designated growth line were drilled to a depth of no more than 0.5 mm below the surface of the valve (Figure 1a: total ~1 mm): the upper prismatic layer is between 2–3 mm in thickness in these modern *S. gigantea* specimens. Care was taken to remain within <0.5 mm of the desired growth line, but toward the edge of the shell this type of sampling technique may homogenize more time than that
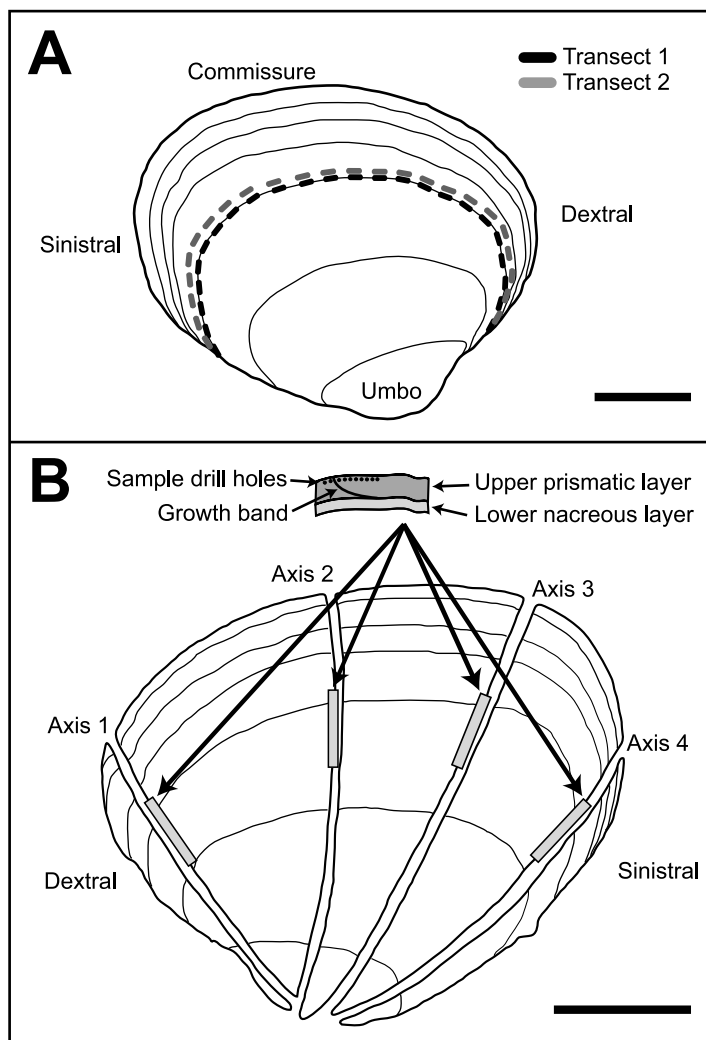
Figure 1. Sampling approaches on a modern Butterclam, *Saxidomus gigantea*, Namu, British Columbia. Scale bars are 2 cm. (a) Hendy-type test on left valve. Transect 1 is on a visible growth band, whereas Transect 2 is off the growth band. (b) Multiaxial growth analysis was completed on the right valve of the same specimen. Note that not all growth lines are depicted on the shell diagram.

sampled along the axis of maximum growth. Sample spacing is provided in Figure 1a.

2.1.2. Multiaxial Growth Analysis

[8] A multiaxial growth analysis was preformed in order to remove sampling errors associated with the edge of the shell and determine if fragmentary segments of the shell can be used to construct seasonality profiles. Rather than using another modern shell, the right valve of the same modern specimen used for the Hendy-type test above was used (Figure 1b). The valve was cross-sectioned four times, with each cut being as perpendicular to the growth lines as possible (axis 3 being the typical cut for sclerochronological investigations). Discrete sub-samples were drilled (distance between samples

was ∼0.6 mm) from the upper prismatic layer using a growth line as a reference point (Figure 1b). Across the designated growth band 10 sub-samples were obtained with 8 samples prior to the growth band (older) and 2 after the growth band (younger). The distances to each sample point along the individual profiles were normalized in order to make a direct comparison between the profiles produced on axes of different length. The normalized distance (d_n) was achieved using the following equation:

$$d_n = \text{distance to point/total axis length}.$$

2.2. Stable-Isotope Analysis

[9] Isotopic analysis was carried out on carbonate powder that was not treated with peroxide or bleach. A common acid-bath ISOCARB system
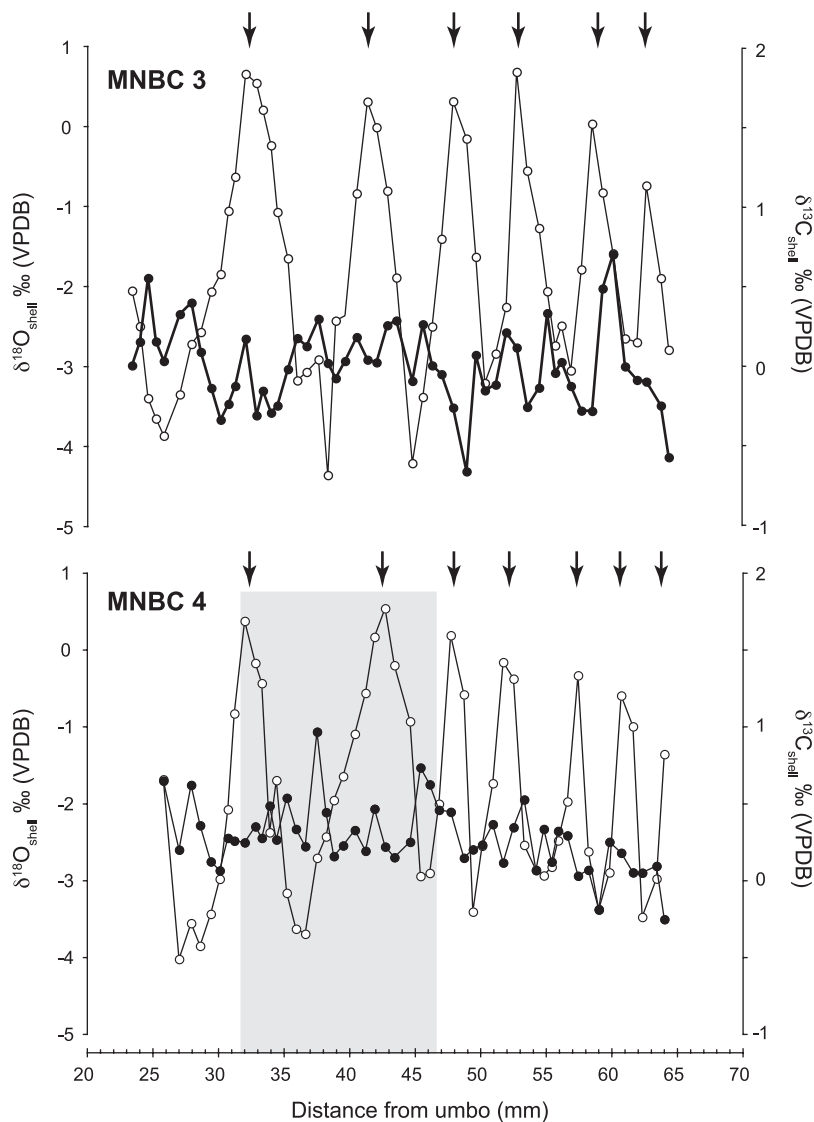
Figure 2. The $\delta^{13}C_{shell}$ (filled) and $\delta^{18}O_{shell}$ (open) results from a typical analysis along the axis of maximum growth (axis 3 in Figure 1b) in two modern *S. gigantea* collected from the same beach at Namu in August 2006. Grey area represents the region analyzed for the multiaxial growth analysis. Arrows point to growth lines.

coupled with a VG OPTIMA isotope-ratio mass-spectrometer was used to generate the isotopic data set. Results are reported in the standard delta (δ) notation relative to Vienna Pee Dee Belemnite (VPDB). Samples were corrected using NBS-19 reference material ($\delta^{13}C = +1.95$‰, $\delta^{18}O = -2.20$‰), which had an analytical precision better than 0.1‰ for both $\delta^{13}C$ and $\delta^{18}O$.

3. Results and Discussion

[10] The profiles of MNBC 3 and MNBC 4 along axis 3 (Figure 1b) are presented in Figure 2. Each of these profiles show distinct cycles in $\delta^{18}O_{shell}$ that exhibit larger spacing at the umbo end, with closer spacing toward the commissure. What is evident in these profiles is that the magnitude of the $\delta^{18}O_{shell}$ tends to decrease with age: a result not found by *Gillikin et al.* [2005]. Cycles within $\delta^{13}C_{shell}$ are not as apparent as $\delta^{18}O_{shell}$, although a minor trend (<0.4‰) toward more negative numbers from the umbo to commissure is recorded.

[11] To illustrate the reproducibility between these two specimens, as shown previously for *Mercenaria mercenaria* by *Elliot et al.* [2003] and *S. gigantea* by *Gillikin et al.* [2005], the x axis of the $\delta^{18}O_{shell}$ profile of one specimen was fixed (MNBC 3) and the other profile (MNBC 4) stretched and condensed along the x axis in order
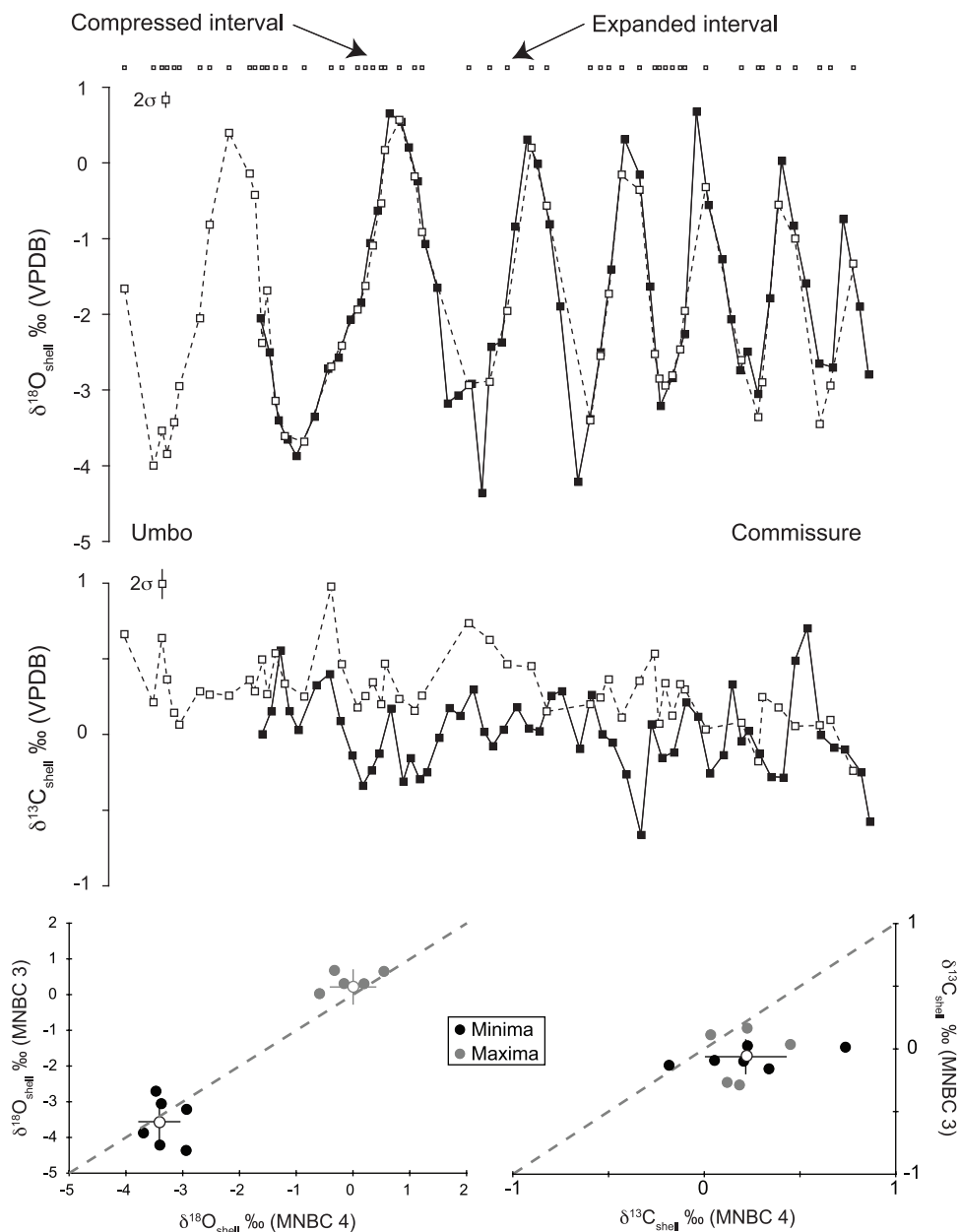
Figure 3. Comparison of $\delta^{13}C_{shell}$ and $\delta^{18}O_{shell}$ from two modern *S. gigantea*. The open symbols represent the shell used in this study (MNBC 4). The smaller open symbols at the top represent sample spacing and thus areas that were compressed or expanded in MNBC 4 to fit the profile of MNBC 3. The two cross-plots at the bottom illustrate the fit between $\delta^{18}O_{shell}$ maxima versus $\delta^{18}O_{shell}$ minima and between $\delta^{13}C_{shell}$ maxima versus $\delta^{13}C_{shell}$ minima. These graphs show how good our comparison is as ideally they should fit on the 1:1 line. The open symbols with crosshairs represent the average and standard deviation of each group.

to produce a comparative curve (Figure 3). The last value for MNBC 4 was deliberately fixed to the nearest $\delta^{18}O_{shell}$ segment of the curve at the commissure, since both shells were collected on the same day and thus they should have the same $\delta^{18}O_{shell}$ value. The different value and trend for the final analyses of each profile may be caused by sampling across finer growth increments, based on

the fact that MNBC 3 is in a mature phase of growth, whereas MNBC 4 is senile (Figure 4). Senile growth is slower and more irregular than mature growth, which leads to a compaction of growth increments toward the commissure. Thus the last point for MNBC 4 may represent a mixture of the last 3 samples recorded in MNBC 3 (i.e., time-averaging [*Goodwin et al.*, 2003a]).
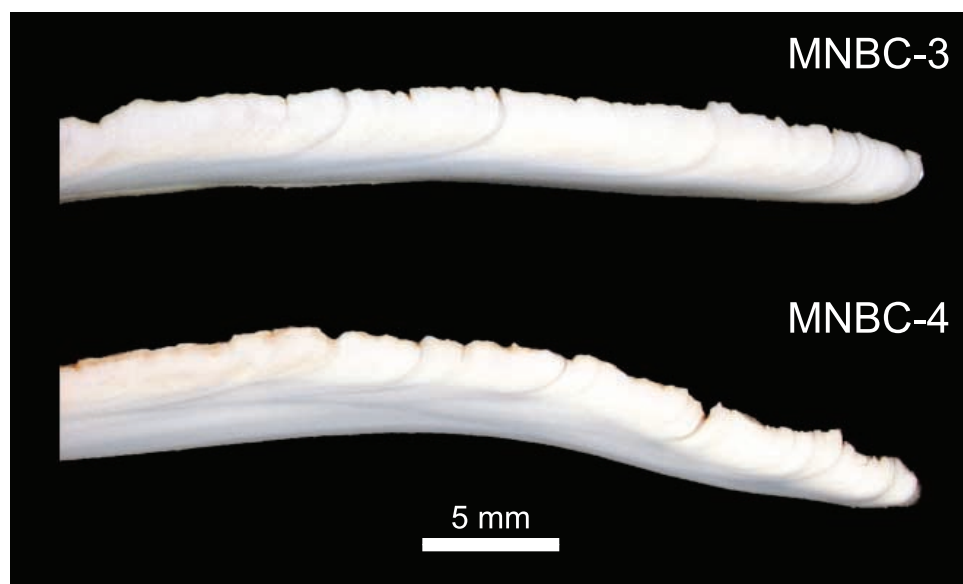
Figure 4. Thin sections of MNBC 3 and MNBC 4. Note that MNBC 3 is classified as mature, whereas MNBC 4 is senile. The disparity between the final set of $\delta^{13}C_{shell}$ and $\delta^{18}O_{shell}$ values is the result of not sampling at high enough resolution in MNBC 4 to capture the same record as that produced in MNBC 3 (see text for discussion).

[12] The reproducibility for $\delta^{18}O_{shell}$ is exceptional, although due to changing growth rates between the specimens and sample spacing some segments of the curve are not represented. Future multiaxial growth analysis should employ regular spacing as that utilized by *Gillikin et al.* [2005]. It is interesting to note that reproducible variability mainly occurs at the most enriched and depleted segments of the profile, which would indicate that each specimen had different levels of tolerance to environmental parameters and/or a result of time averaging. The seasonal magnitude in $\delta^{18}O_{shell}$ decreases through the lifespan of both individuals, and may be related to environmental and/or biological factors, or even a time-averaging effect due to sampling [*Goodwin et al.*, 2003a]. Reproducibility in $\delta^{13}C_{shell}$ was not as good as $\delta^{18}O_{shell}$; however, there are segments along the profile where $\delta^{13}C_{shell}$ is very reproducible and show the same trends in some years. A similar finding was reported by *Gillikin et al.* [2005]. The differences in $\delta^{13}C_{shell}$ are possibly the result of the individuals having varying levels of respired carbon incorporated into the shell [*McConnaughey et al.*, 1997], since they were living in the same area and habitat.

3.1. Hendy-Type Test

[13] Results from the traditional Hendy-type test are provided in Figure 5. Total variability in $\delta^{18}O_{shell}$ on the growth increment (Transect 1) and off the growth increment (Transect 2) was greater than 2.5‰. All the data along both transects produced relatively large standard deviations (Transect 1, $-0.39‰ \pm 0.76‰$; Transect 2, $+0.11‰ \pm 0.48‰$). Removing the sinistral portions of the profile (3 samples from Transect 1; 1 sample from Transect 2) the standard deviations are reduced by half (Transect 1, $-0.13‰ \pm 0.34‰$; Transect 2, $+0.20‰ \pm 0.21‰$). The increased variability at the sinistral portion could be the result of the sampling process, but it is interesting to note that $\delta^{13}C_{shell}$ shows no significant variability at this margin.

[14] $\delta^{13}C_{shell}$ exhibits far less variability across the entire sample set (Transect 1, $+0.14‰ \pm 0.15‰$; Transect 2, $+0.03‰ \pm 0.09‰$). Unlike $\delta^{18}O_{shell}$, $\delta^{13}C_{shell}$ shows greater variability on the dextral margin of the shell, but still within analytical and sampling uncertainty. Removing the last 5 samples from the dextral margins reduces the variability in Transect 1 by half but does not reduce the variability in Transect 2. Again this may be associated with the sampling process, as noted by the overlap of isotopic values at the sinistral and dextral margins.

[15] *Klein et al.* [1996] report significant $\delta^{13}C_{shell}$ variation (between 0.5‰ to 0.8‰) around the margins of *M. trossulus* in comparison to the central portions of the shell. In comparison, $\delta^{18}O_{sh-shell}$ recorded very little variation along each transect (0.2‰ to 0.4‰). However, this study only
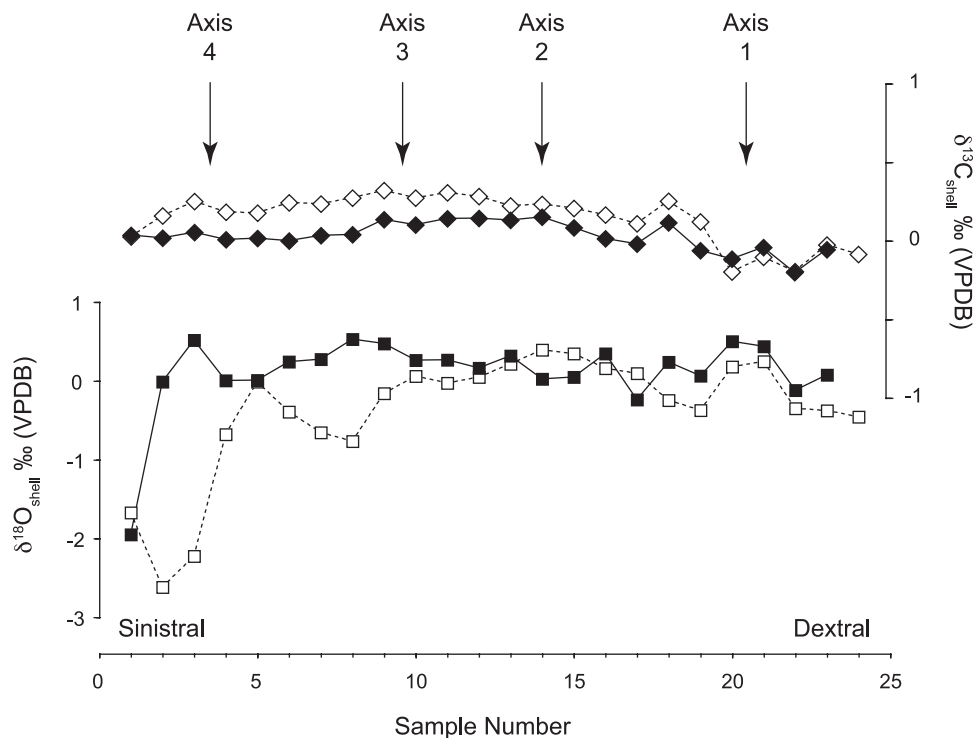
Figure 5. The $\delta^{13}C_{shell}$ (diamonds) and $\delta^{18}O_{shell}$ (squares) results from the Hendy-type test on *S. gigantea*, MNBC 4 (Figure 1a). Transect 1 (on growth line), open symbols; Transect 2 (off growth line), filled symbols. Arrows point to approximate positions for the multiaxial growth analysis (see Figure 1b). There is no significant difference (*t* test) between the last five $\delta^{13}C_{shell}$ results from the dextral margin and the remainder of the data set.

analyzed 3 to 5 samples along each transect around the shell, and hence the variability reported may be a reflection of errors in sampling. *Klein et al.* [1996] explain the variability in $\delta^{13}C_{shell}$ around the margins as a metabolic activity resulting in non-equilibrium effects in comparison to seawater. On the basis of the data in this study, it would indicate the opposite in that $\delta^{13}C_{shell}$ is in equilibrium around the growth line of *S. gigantea*, although $\delta^{18}O_{shell}$ may not be in equilibrium at the sinistral margin.

3.2. Multiaxial Growth Analysis

[16] A traditional sclerochronological transect of the shell was performed along the axis of maximum growth from which 51 samples were analyzed (Figure 2). The multiaxial growth analysis of three other slices around a prominent growth line (grey region in Figure 1b) produces excellent reproducibility for $\delta^{18}O_{shell}$, but not for $\delta^{13}C_{shell}$ (Figure 6). Total variation in $\delta^{13}C_{shell}$ values within all axes was 1.1‰ with the highest value associated with axis 3 and the lowest with axis 2. The largest range (0.8‰) is seen in axis 3. What is apparent with this comparison is that when $\delta^{18}O_{shell}$ values

are at their lowest the variability in $\delta^{13}C_{shell}$ is greatest. However, when $\delta^{18}O_{shell}$ approach more positive values, $\delta^{13}C_{shell}$ values show less variability among all axes. It is interesting to observe that axis 1 and 2 (dextral margin) exhibit the highest covariance in both $\delta^{13}C_{shell}$ and $\delta^{18}O_{shell}$, in comparison to the other axes. It is suggested that a complex interaction between biological effects, such as metabolic activity (i.e., respiration [*McConnaughey et al.*, 1997]), and environmental effects (i.e., ecosystem metabolic activity) is the cause of the variation in $\delta^{13}C_{shell}$, although subtle changes in growth rate around the margin may also be a factor.

[17] All four axes have reproducible profiles for $\delta^{18}O_{shell}$ when normalized for variable axial lengths. This suggests that any transect through a shell can be used for seasonality analysis, although if using shell material closer to the margins high-resolution sampling must be achieved in order to capture the full cycle in $\delta^{18}O_{shell}$. The minor differences in $\delta^{18}O_{shell}$ profiles (Figure 6) may be a result of the normalizing procedure and/or potential differences in $\delta^{18}O_{shell}$ around a growing margin (Figure 5, sinistral margin). However, the range in
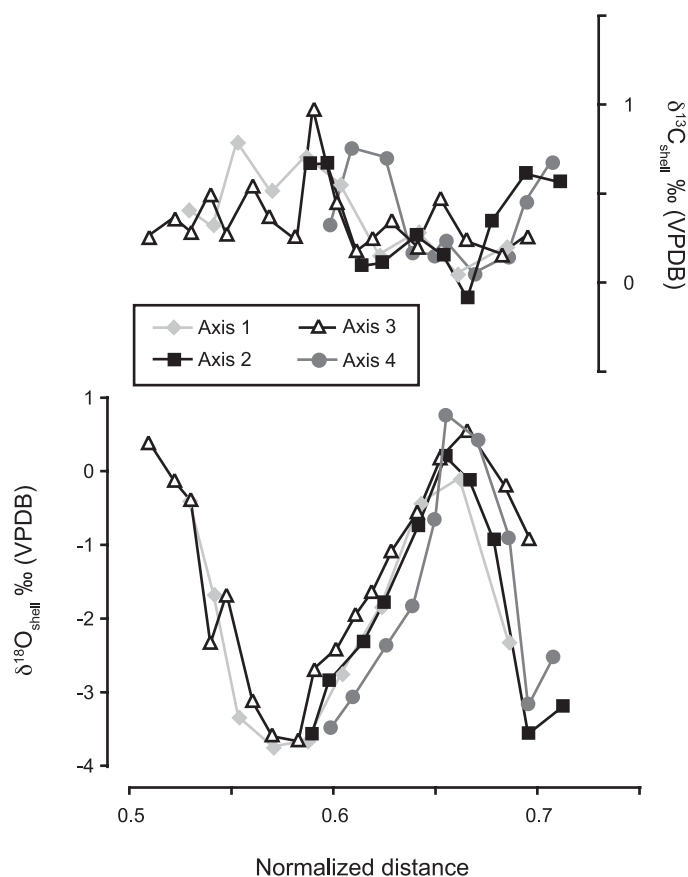
Figure 6. The $\delta^{13}C_{shell}$ and $\delta^{18}O_{shell}$ results from a multiaxial growth analysis in *S. gigantea*, MNBC 4 (see Figure 1b). See text for discussion on determining normalized distance.

values according to normalized distance is likely the result of the sampling process, because all isotopic samples are taken as discrete aliquots and not continuously sampled. As a result it is not possible to sample all portions of the isotopic profile using the drilling techniques employed in this study. A future approach would be to take equidistance micro-samples on each axis between two growth lines, and then normalize to growth rate between years. A continuous milling method, such as that used by *Schöne et al.* [2006] would be ideal.

[18] Differences in the portion of the profile used in this study are governed by the length of the axis. In smaller axial lengths (e.g., margins) the isotopic record is recorded through less material and therefore the record is condensed in comparison to axes of longer length (e.g., axis 3). For this reason, after normalization of the data the shortest axis (axis 1) records more of the seasonal profile per unit distance. Axis 3 is the longest, and therefore is typically used in sclerochronological studies to generate a profile of the whole shell. However,

we have extended the normalization technique back an extra 8 samples in axis 3 in order to encompass the length of the profile recorded in axis 1 (Figure 6). The ability to sample more time along axis 3 reveals a small fluctuation at 0.54 on the normalized distance scale, which is not recorded in the shorter axis (e.g., axis 1). To generate a record with the highest resolution in order to show subtle changes it is advisable to analyze the axis of maximum growth (axis 3). If low-resolution or time-averaged isotopic values are sufficient, which could be more economical in larger bivalve species, it is advisable to analyze the shorter axis.

4. Conclusions and Implications

[19] Seasonal profiles generated from two individual *S. gigantea* specimens from Namu, British Columbia show excellent reproducibility in $\delta^{18}O_{shell}$. $\delta^{13}C_{shell}$ from these two individuals show that during earlier growth stages there was good covariance, although the reproducibility

of absolute $\delta^{13}C_{shell}$ was poor. Other periods of growth show good reproducibility; however, the covariance was reduced. Hendy-type tests from an individual used to generate one of the above profiles produced excellent reproducibility along a growth horizon in $\delta^{13}C_{shell}$, whereas $\delta^{18}O_{shell}$ produced greater variability especially at the sinistral margin. Multiaxial growth analysis results show that similar seasonal $\delta^{18}O_{shell}$ profiles are recorded in all portions of the shell. $\delta^{13}C_{shell}$ profiles did not exhibit very reproducible profiles, except in axis 1 and 2. As previously suggested, metabolic processes affect the variability in $\delta^{13}C_{shell}$, whereas $\delta^{18}O_{shell}$ is controlled primarily by environmental changes independent of internal metabolic activity, hence the poor reproducibility in $\delta^{13}C_{shell}$ in comparison to $\delta^{18}O_{shell}$. Therefore, provided sample spacing is matched to axial length, using a normalization process, shell fragments can be accurately used to investigate seasonal profiles in bivalves. $\delta^{18}O$ profiles of shells from a single site and timeframe can be accurate recorders of seasonal changes that also show excellent reproducibility. Fragments from whole shells can also be used to generate seasonality profiles, which is important when investigating shell-poor or fragmented shells from archaeological deposits (e.g., shell middens). Multiaxial growth analysis using $\delta^{18}O_{shell}$ profiles could prove to be an excellent method in which to investigate the types [*Goodwin et al.*, 2003b] and rates of growth in a shell.

Acknowledgments

References

Carré, M., I. Bentaleb, D. Blamart, N. Ogle, F. Cardenas, S. Zevallos, R. M. Kalin, L. Ortlieb, and M. Fontugne (2005), Stable isotopes and sclerochronology of the bivalve Mesodesma donacium: Potential application to Peruvian paleoceanographic reconstructions, *Palaeogeogr. Palaeoclimatol. Palaeoecol.*, *228*, 4–25.

Elliot, M., P. B. deMenocal, B. K. Linsley, and S. S. Howe (2003), Environmental controls on the stable isotopic composition of *Mercenaria mercenaria*: Potential application to paleoenvironmental studies, *Geochem. Geophys. Geosyst.*, *4*(7), 1056, doi:10.1029/2002GC000425.

Gillikin, D. P., F. De Ridder, H. Ulens, M. Elskens, E. Keppens, W. Baeyens, and F. Dehairs (2005), Assessing the reproducibility and reliability of estuarine bivalve shells (*Saxidomus giganteus*) for sea surface temperature reconstruction: Implications for paleoclimate studies, *Palaeogeogr. Palaeoclimatol. Palaeoecol.*, *228*, 70–85.

Goodwin, D., B. Schöne, and D. Dettman (2003a), Resolution and fidelity of oxygen isotopes as paleotemperature proxies in bivalve mollusk shells: Models and observations, *Palaios*, *18*, 110–125.

Goodwin, D. H., L. C. Anderson, and P. D. Roopnarine (2003b), Observations on corbulid growth and their evolutionary significance, *Geol. Soc. Am. Abstr. Programs*, *35*(6), 318.

Hendy, C. H. (1971), The isotopic geochemistry of speleothems. Part 1. The calculation of the effects of different modes of formation on the isotopic composition of speleothems and their as paleoclimatic indicators, *Geochim. Cosmochim. Acta*, *35*, 801–824.

Klein, R. T., K. C. Lohmann, and C. W. Thayer (1996), Sr/Ca and $^{13}C/^{12}C$ ratios in skeletal calcite of *Mytilus trossulus*: Covariation with metabolic rate, salinity, and carbon isotopic composition of seawater, *Geochim. Cosmochim. Acta*, *60*, 4207–4221.

Krantz, D. E., D. F. Williams, and D. S. Jones (1987), Ecological and paleoenvironmental information using stable isotope profiles from living and fossil mollusks, *Palaeogeogr. Palaeoclimatol. Palaeoecol.*, *58*, 249–266.

Lauritzen, S., and J. Lundberg (1999), Speleothems and climate: A special issue of *The Holocene*, *Holocene*, *9*, 643–647.

McConnaughey, T. A., J. Burdett, J. F. Whelan, and C. K. Paull (1997), Carbon isotopes in biological carbonates: Respiration and photosynthesis, *Geochim. Cosmochim. Acta*, *61*, 611–622.

Rosenberg, G., and W. W. Hughes (1991), A metabolic model for the determination of shell composition in the bivalve mollusc, *Mytilus edulis*, *Lethaia*, *24*, 83–96.

Schöne, B., D. Rodland, J. Fiebig, W. Oschmann, D. Goodwin, K. Flessa, and D. Dettman (2006), Reliability of multi-taxon, multi-proxy reconstructions of environmental conditions from accretionary biogenic skeletons, *J. Geol.*, *114*, 267–285.

Shackleton, N. J. (1973), Oxygen isotope analysis as a means of determining season of occupation of prehistoric midden sites, *Archaeometry*, *15*, 133–141.